



No.97-203

JSME CENTENNIAL GRAND CONGRESS

Proceedings of International Conference on Fluid Engineering VOL. I ICFE '97

July 13 - 16, 1997

Tokyo International Forum, Tokyo, Japan

Organized by Fluid Engineering Division, JSME

Co-organized by Fluids Engineering Division, ASME

Thermal and Fluids Engineering Division, KSME



The Fluid Engineering Division

THE JAPAN SOCIETY OF MECHANICAL ENGINEERS

Investigation of the Periodic Structure of Longitudinal Vortices Shedding from Criss-Cross Circular Cylinders Applying Lock-in Phenomenon

Atsushi NAKAHARA, NISSEI ASB Machine co., ltd., 4586-3, Koo Komoro, Nagano, 384, JAPAN
Tsutomu TAKAHASHI, Nagaoka University of Technology, 1603-1, Kamitomioka, Nagaoka, Niigata, 940-21, JAPAN
László BARANYI, Nagaoka University of Technology
Masataka SHIRAKASHI, Nagaoka University of Technology

ABSTRACT

It was reported in earlier papers by the present authors that longitudinal vortices are shed periodically from two cylinders in a cruciform arrangement with a gap s between them, placed in an otherwise uniform flow. The longitudinal vortices can cause flow-induced vibration of the upstream cylinder in the case when it is supported elastically. It was found that the vortex shedding synchronizes with the cylinder oscillation (lock-in phenomenon) when the amplitude of oscillation is large. When the gap-to-diameter ratio $s/d \leq 0.25$ trailing vortices, and when $0.25 \leq s/d \leq 0.5$ necklace vortices are shed periodically.

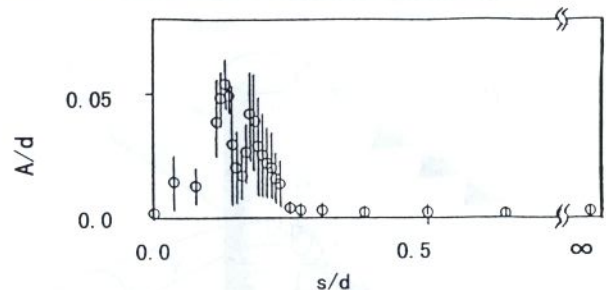
The aim of this work is to investigate the periodic structure of the vortices which are responsible for the longitudinal vortex excitation. Since the lock-in phenomenon makes the periodicity of vortex shedding more regular and the displacement signal of upstream cylinder works as a precise clock, the periodic structure of longitudinal vortices is extracted successfully by applying the phase averaging technique.

1 INTRODUCTION

The interference effect of neighboring bodies on the oscillation of a cylindrical body in cross flow is of practical importance because it can induce undesirable oscillations [1,2]. Compared with flows around two-dimensional arrangements (e.g. [3]), papers concerning the flow around two cylinders in a cruciform arrangement are rather few in spite of the fact that there are many equipment in plants and laboratories with such an arrangement. It was reported by the present authors [4,5] that a large oscillation, as shown in Fig. 1, can be induced on an elastically supported cylinder when another cylinder is set downstream in a cruciform arrangement. When the gap s between the two cylinders was varied while the free stream velocity U was fixed at 8 m/s, a new oscillation appeared in the range of $s/d < 0.25$. It was suggested that this large oscillation of the upstream cylinder is due to periodic shedding of either the trailing vortices or the necklace vortices, as illustrated in Fig. 2. These figures were drawn based on measurements of pressure distribution on the upstream cylinder surface [6,7], the x component of velocity fluctuation [7,8], the observations on the mean flow [9,10], and flow visualization in a water tunnel [11]. Since both types of these vortices have axes parallel to the free stream flow, we called this new oscillation "longitudinal vortex excitation".

The aim of this work is to investigate the periodic structure of the vortices which are responsible for the

longitudinal vortex excitation. The upstream cylinder was oscillated mechanically with a controlled frequency and amplitude in a wind-tunnel to make the vortex shedding synchronized with the cylinder oscillation. Since the lock-in phenomenon makes the periodicity of vortex shedding more regular, further the displacement signal of the upstream cylinder works as a precise clock, the three-dimensional periodic structure of longitudinal vortices can be discerned successfully by applying the phase averaging technique using the cylinder displacement as the reference signal. Preceding this experiment, conditions for the lock-in phenomenon were investigated by changing the flow velocity, and the frequency and amplitude of the cylinder oscillation.



Free stream velocity $U = 8$ m/s
Cylinder diameter $d = 26$ mm
Natural frequency of the upstream cylinder $f_c = 24$ Hz

Fig. 1 Variation of non-dimensional oscillation amplitude A/d with gap s/d

2 EXPERIMENTAL APPARATUS & PROCEDURE

The arrangement of the cylinders and the coordinate system are shown in Fig. 2. Cylinder diameters d are 26 mm for wind tunnel and 10 mm for water tunnel experiments, respectively. Measurements for Reynolds numbers above 2500 (Reynolds number $Re = Ud/\nu$; ν kinematic viscosity of the fluid) were carried out in a wind tunnel with hot wire anemometers (HWA), and for $500 < Re < 2100$ in a water tunnel with a hot film anemometer (HFA). Experiments for the trailing vortex were carried out at $s/d = 0.08$, and those for the necklace vortex at $s/d = 0.28$, because the periodicity can most clearly be observed at these values [8].

Velocity signals obtained by HWA or HFA were analyzed by FFT to obtain the vortex shedding frequency f_v . The flow in a water tunnel was visualized by introducing

dye in order to be able to observe the configuration of the vortices and also to determine f_v . The influence of the upstream cylinder oscillation on the vortex shedding was investigated by oscillating the cylinder mechanically. The free stream velocity U , the oscillation amplitude A and the oscillation frequency f_c of the upstream cylinder were varied independently, and the ranges of these variables for the "lock-in phenomenon" of the longitudinal vortices were investigated.

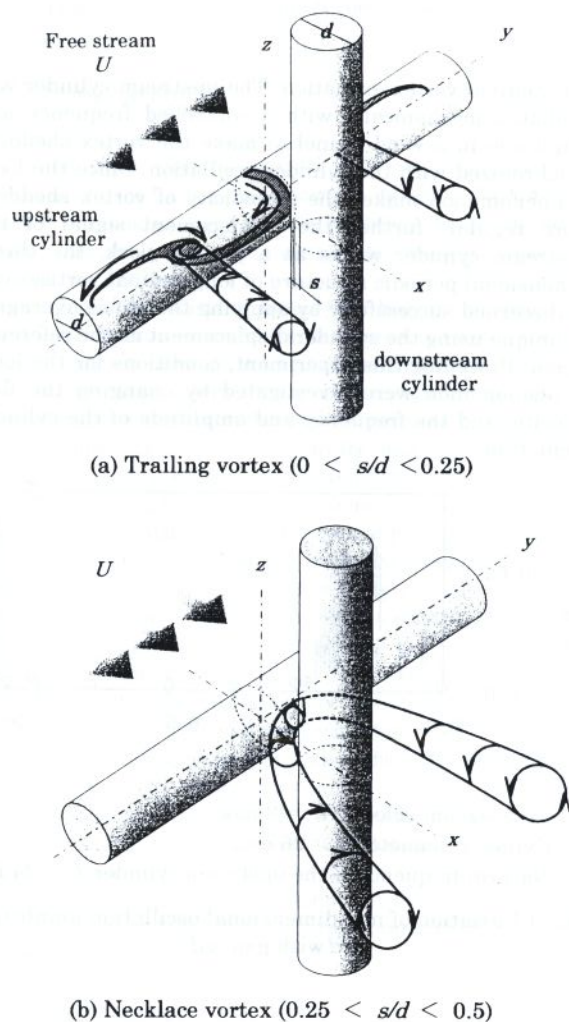


Fig. 2 Vortex models and coordinate system

3 PRINCIPLE OF THE PHASE AVERAGING TECHNIQUE UTILIZING LOCK-IN PHENOMENON

To make the periodic change of the flow field caused by the longitudinal vortex shedding discernible from the data obtained by HWA, the following procedure was applied.

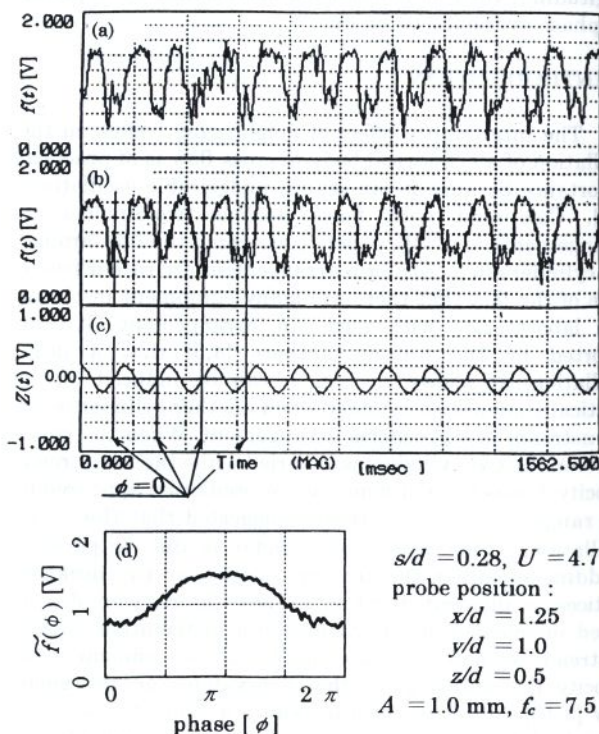
Fig. 3-(a) shows an oscillogram of an output signal of the HWA for the case of fixed upstream cylinder. It is obvious that the velocity fluctuation is caused by the vortex shedding. Although the probe was set at a point where the periodicity was clearly observed, the signal is subjected to considerable noise.

To learn more about the periodic structure of the vortices requires the thorough knowledge of the velocity field at an arbitrary phase of a period of vortex shedding.

The measurements of velocity components u , v and w were carried out point by point, and time t for a velocity signal was correlated with the phase ϕ within a period in this work. To make this correlation precise, the upstream cylinder was oscillated with a fixed amplitude A and frequency f_c to make the vortex shedding synchronize with the oscillation. We used the cylinder displacement as the reference signal. Oscillograms (b) and (c) in Fig. 3 show the velocity signal and the displacement signal Z of the upstream cylinder detected simultaneously under the same conditions as in case (a), not considering the cylinder oscillation. It can be seen that the velocity signal synchronizes with the cylinder displacement Z , i.e. the lock-in phenomenon does occur, confirming that Z can work as the reference signal. Although the periodicity of the velocity signal in (b) is considerably better than in (a), the velocity signal (b) is still affected by disturbance due to flow turbulence. This disturbance can largely be eliminated by taking an average of the velocity signal in a period. The displacement signal Z is used as a "clock" to identify every period, and the time at which the phase $\phi = 0$ is defined as the point where $Z = 0$ while $dZ/dt > 0$, as illustrated in Fig. 3-(c). Once an arbitrary time is correlated with a phase ϕ in a period, the phase average of a fluctuating signal $f(t)$ synchronized with Z is defined as

$$\tilde{f}(\phi) = \frac{1}{N} \sum_{i=1}^N f_i(\phi),$$

where i is the period-number and N is the number of the periods.



(a) Fluctuating signal $f(t)$ for a fixed system
 (b) Fluctuating signal $f(t)$ for an oscillation system
 (c) Displacement signal $Z(t)$ of the upstream cylinder
 (d) Phase averaged signal $\tilde{f}(\phi)$

Fig. 3 Sample of signals and their analyses

The sampling time for the digitalization was 1/100 of a period, and the number of periods N for the averaging was 64 in the results presented later.

necklace vortex increases with Re in the region $500 < Re < 4000$, and is constant of around 0.045 in the region $Re > 4000$. When $Re < 500$ the necklace vortex shedding was not clearly observed.

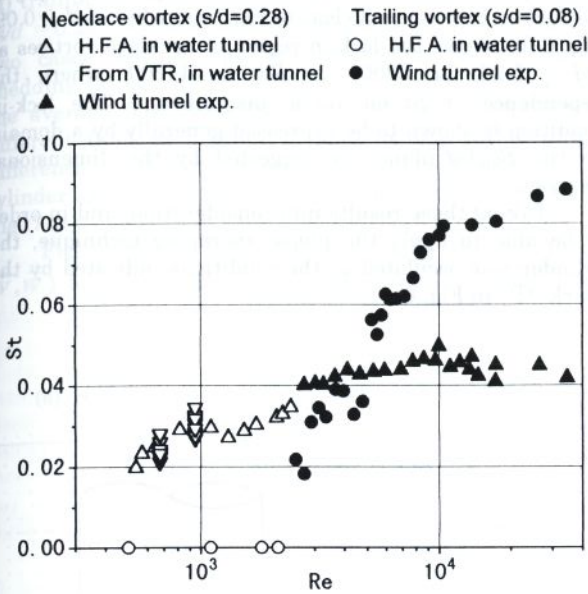
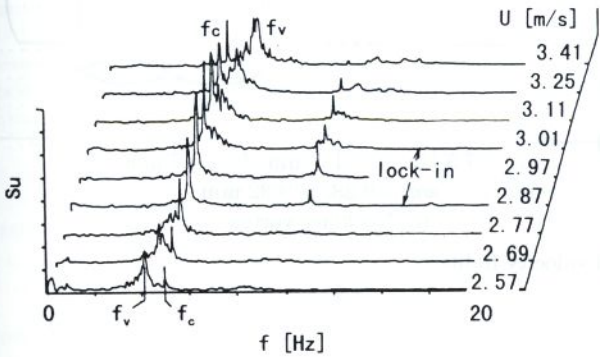


Fig. 4 Relationship between St and Re for the fixed system



Probe position : $x/d = 1.25, y/d = 1.0, z/d = 0.25$
 $s/d = 0.28, f_c = 5 \text{ Hz}, A/d = 0.096$

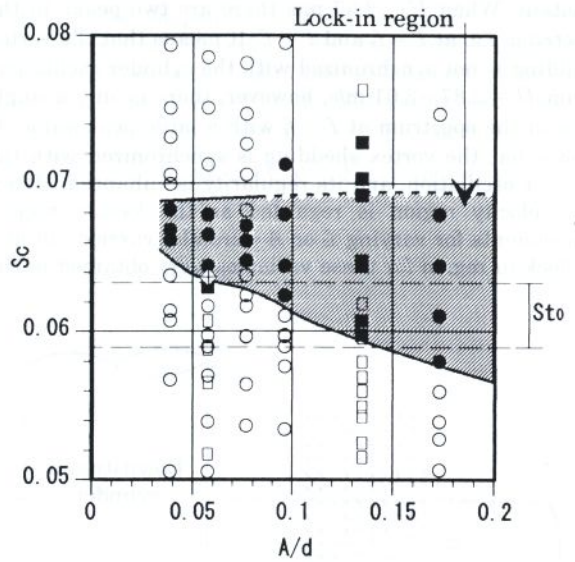
Fig. 5 Linear spectra of velocity component u for various U

4 RESULTS AND DISCUSSION

4.1 Dependence of Strouhal number of the vortices on Reynolds number

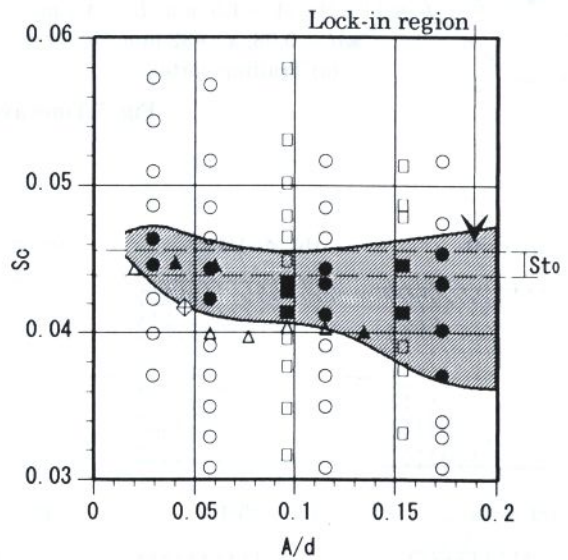
Fig. 4 shows the relationship between the Strouhal number St ($= f_c d/U$) and the Reynolds number Re when the upstream cylinder is fixed. St for the trailing vortex increases with Re in the region $2500 < Re < 10000$, and is practically constant at a value of $0.08 \sim 0.09$ when $Re > 10000$. Open circles at $St = 0$ in the region $500 < Re < 2100$ in the figure show the fact that the vortices are formed steadily but not shed periodically. St for the

\diamond : velocity measurement condition for phase averaging



	no lock-in	lock-in	Re
f_c varied	\circ	\bullet	6600
U varied	\square	\blacksquare	5000~17000

(a) trailing vortex



	no Lock-in	Lock-in	Re
f_c varied	\circ	\bullet	4300, 7800
U varied	\square	\blacksquare	2800~14200
A varied	\triangle	\blacktriangle	5000

(a) necklace vortex

Fig. 6 Lock-in regions for longitudinal vortices

4.2 Lock-in phenomenon of longitudinal vortices

It was confirmed in a previous work of the present authors [4] that the shedding frequency f_v of longitudinal vortices can coincide with the upstream cylinder oscillation frequency f_c over a certain range of free stream velocity U . Fig. 5 shows the linear spectra of the velocity u measured at a point near the crossing for various U values while the cylinder oscillation amplitude A and frequency f_c are kept constant. When $U = 2.57$ m/s there are two peaks in the spectrum, i.e. at $f = f_v$ and $f = f_c$. It means that the vortex shedding is not synchronized with the cylinder oscillation. When $U = 2.87 \sim 3.01$ m/s, however, there is only a single peak in the spectrum at $f = f_c$ with a large peak value. It shows that the vortex shedding is synchronized with the cylinder oscillation, and its regularity is enhanced. Hence this velocity region is regarded as the lock-in region. Experiments for varying f_c or A were also carried out and the lock-in region for these variables were obtained in the

same way. The lock-in region obtained for trailing vortices at $s/d = 0.08$ for $5000 < Re < 17000$ is shown in terms of non-dimensional parameters $Sc = f_c d/U$ and A/d in Fig. 6-(a). In this Re number domain the dependence of St on Re is significant as shown in Fig. 4. The upper boundary of the lock-in region is not clear in Fig. 6-(a) when $A/d > 0.09$. Fig. 6-(b) shows the lock-in region of necklace vortices at $s/d = 0.28$ for $2800 < Re < 14200$, where the dependence of St on Re is insignificant. The lock-in condition is shown to be expressed generally by a domain on the $Sc-A/d$ plane, as suggested by the dimensional analysis.

Taking these results into consideration, and in order to be able to apply the phase averaging technique, the cylinder was oscillated at the conditions indicated by the mark \diamond in Fig. 6.

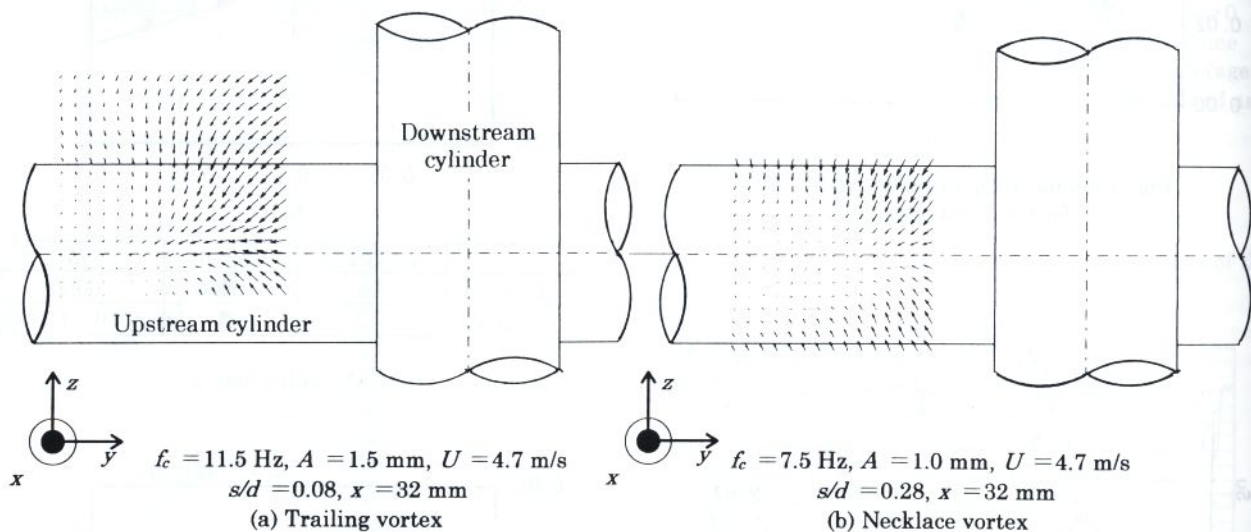


Fig. 7 Time averaged velocity fields

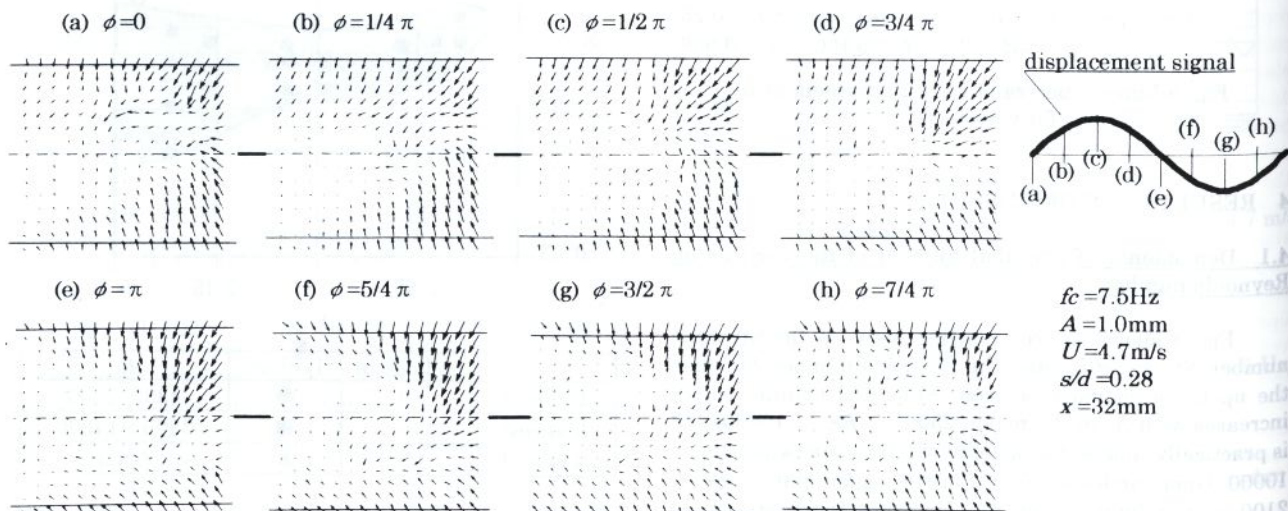


Fig. 8 Phase averaged velocity fields induced by necklace vortices

4.3 Periodic change of the velocity field

Fig. 7 shows the time averaged velocity fields (\bar{v}, \bar{w}) on a $y-z$ plane ($x = 32 \text{ mm}$) viewed from downstream for (a) trailing vortices ($s/d = 0.08$), and (b) necklace vortices ($s/d = 0.28$). Areas of measurements are different for the two cases because the areas affected by the vortex shedding are also different [8]. It can be seen in Fig. 7 that the average flow fields for the two cases are definitely different from each other in spite of the rather slight difference in the gap s . A strong secondary flow along the cylinder axis due to the trailing vortex can be observed in Fig. 7-(a).

Fig. 8 shows the phase averaged velocity fields (\tilde{v}, \tilde{w}) for $s/d = 0.28$ in a complete period obtained for

different angles ϕ , also viewed from downstream direction. The periodic nature of the change in the velocity field in a plane perpendicular to the free stream flow can be made discernible successfully by applying the phase averaging technique. The velocity patterns during $0 < \phi < \pi$ ((a)-(d)) and $\pi < \phi < 2\pi$ ((e)-(h)) seem to be symmetric about the plane $z = 0$ with respective counterpart with a phase shift of π .

The longitudinal vortices induce periodic fluctuation of the velocity components in a plane perpendicular to the free stream flow. Therefore, the fluid motion associated with the periodic shedding of the longitudinal vortices can most clearly be observed by the fluctuating component of vector (\tilde{v}, \tilde{w}) in a $y-z$ plane. This is attained by subtracting $\langle \bar{v}, \bar{w} \rangle$ from (\tilde{v}, \tilde{w}). Fig. 9 shows an example

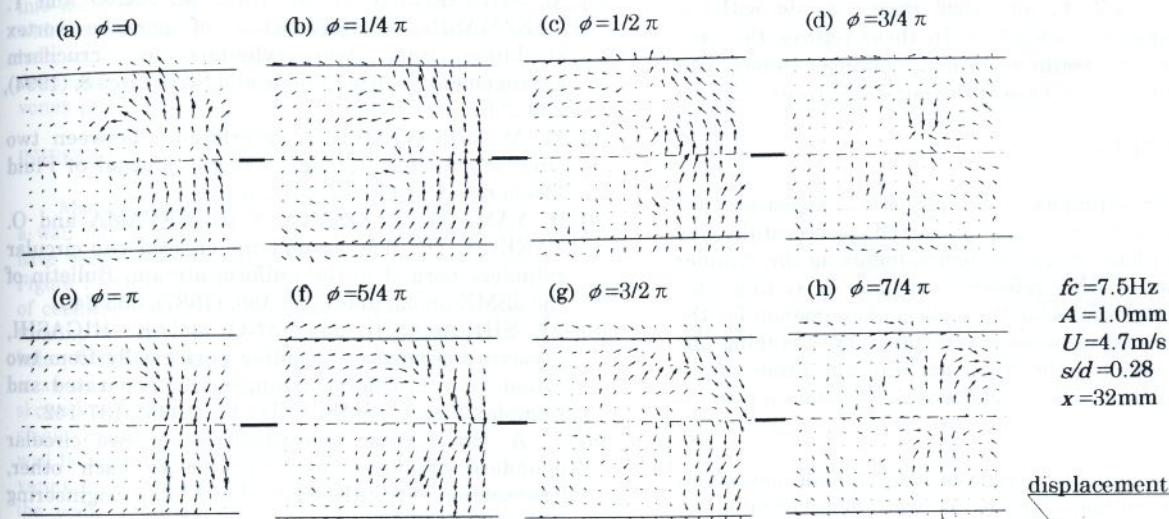


Fig. 9 Fluctuating velocity fields induced by necklace vortices

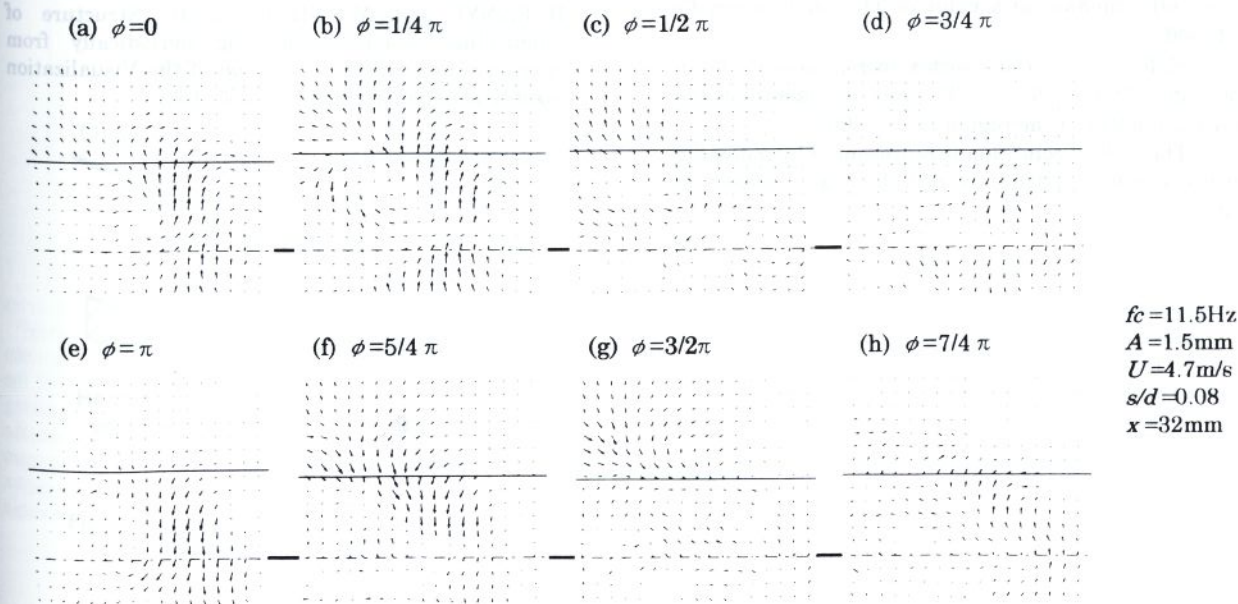


Fig. 10 Fluctuating velocity fields induced by trailing vortices

of such fluctuating velocity fields ($\tilde{v} - \bar{v}, \tilde{w} - \bar{w}$) for the necklace vortices obtained from results shown in Figures 7-(b) and 8. During $0 < \phi < 1/2 \pi$ counterclockwise (ccw) rotation dominates the flow field. For $1/2 \pi < \phi < \pi$ this ccw rotation gradually decays, and clockwise (cw) rotation appears and dominates for $\pi < \phi < 3/2 \pi$. For $3/2 \pi < \phi < 2 \pi$ the cw rotation gradually decays. On the whole it is verified that the periodic change of the flow field is induced by the periodic shedding of the necklace vortices, which are shed anti-phase on $+z$ and $-z$ sides. In these figures, the area influenced by the necklace vortex shedding extends around the plane $z = 0$ behind the upstream cylinder.

Fig. 10 shows the fluctuating velocity fields ($\tilde{v} - \bar{v}, \tilde{w} - \bar{w}$) for the trailing vortices obtained in the same way as the necklace vortices. Although the rotating motion is less clear than that in Fig. 9, it can be seen that the trailing vortices shed from $-z$ side with ccw rotation during $0 < \phi < 1/2 \pi$, and shed from $+z$ side with cw rotation during $\pi < \phi < 3/2 \pi$. In these figures the area influenced by the trailing vortex shedding extends over larger area than in the case of the necklace vortex.

5 CONCLUSION

The three-dimensional periodic structure of longitudinal vortices was extracted successfully by applying the phase averaging technique using the cylinder displacement as the reference signal. Preceding this experiment, conditions for the lock-in phenomenon for the longitudinal vortices were investigated by changing the free stream velocity, the frequency and amplitude of the cylinder oscillation. The conclusions can be summarized as follows.

- (1) The periodic change of velocity field caused by the longitudinal vortices is well demonstrated by applying the phase averaging technique using the cylinder displacement as the reference signal.
- (2) In the region $500 < Re < 2100$ the trailing vortices are formed steadily ($St = 0$). In the region $2500 < Re < 10000$ St increases with Re , and it is practically constant at a value of $0.08 \sim 0.09$ when $Re > 10000$.
 St for the necklace vortex increases with Re in the region $500 < Re < 4000$, and is constant value of around 0.045 in the region $Re > 4000$.
- (3) The lock-in condition is represented by a domain on the non-dimensional $Sc-A/d$ plane as shown in Fig. 6.

REFERENCES

- [1] A. BOKAIN and F. GEOOLA, Wake-induced galloping of two interfering circular cylinders, *Journal of Fluid Mechanics* 146, (1994), 383-415.
- [2] B. H. L. GOWDA and D. R. PRABHU, Interference effects on the flow-induced vibration of a circular cylinder, *Journal of Sound and Vibration*. 112-3, (1987), 487-502.
- [3] P. W. BEARMAN and A. J. WADCOCK, The interaction between a pair circular cylinders normal to a stream, *Journal of Fluid Mechanics* 61, (1973), 499-511.
- [4] M. SHIRAKASHI, K. MIZUGUCHI and H. M. BAE, Flow-induced excitation of an elastically supported cylinder caused by another located downstream in cruciform arrangement, *Journal of Fluids and Structures* 3, (1989), 595-607.
- [5] M. SHIRAKASHI, H. M. BAE, M. SANO and T. TAKAHASHI, Characteristics of periodic vortex shedding from two cylinders in cruciform arrangement, *Journal Fluids and Structures* 8, (1994), 239-256.
- [6] M. M. ZDRAVKOVICH, Interference between two circular cylinders forming a cross, *Journal of Fluid Mechanics* 128, (1983), 231-246.
- [7] H. YAMADA, H. OSAKA, Y. KAGEYAMA and O. TAKEDA, The flow around the crossed two circular cylinders normal to the uniform stream, *Bulletin of the JSME (in Japanese)* 53-486, (1987), 333-340.
- [8] M. SHIRAKASHI, M. SANO and K. HIGASHI, Structure of vortices shedding periodically from two cylinders in cruciform arrangement, *Separated and Complex Flows*, ASME, FED 217, (1995), 137-142.
- [9] T. A. FOX, Wake characteristics of two circular cylinders arranged perpendicular to each other, *Transaction of ASME, Journal of Fluids Engineering* 113, (1991), 45-50.
- [10] T. A. FOX, Interference in the wake of two Square-section cylinders arranged perpendicularly to each other, *Journal of Wind Engineering and Industrial Aerodynamics* 40, (1992), 75-92.
- [11] F. HOSAKA, A. NAKAHARA, T. TAKAHASHI, L. BARANYI and M. SHIRAKASHI, Structure of longitudinal vortices shedding periodically from cruciform two cylinders, *Journal of the Visualization Society of Japan* 16-2, (1996), 159-162.